Spallation Neutron Source Effects in a Sub-Critical System

P. Seltborg*

Department of Nuclear and Reactor Physics, Royal Institute of Technology, Stockholm, Sweden

R. Jacqmin

CEA Cadarache, SPRC/LEPh Bat. 230, 13108 Saint-Paul-lez-Durance, France

Abstract – *Numerical simulations of a sub-critical system coupled to a neutron spallation source (1000 MeV protons impinging on a lead target) have been performed with the Monte Carlo code MCNPX and the deterministic code system ERANOS. The investigations have focused on the determination of the source neutron efficiency, φ^*, i.e. the ratio of the average importance of external source neutrons to the average importance of fission neutrons. The calculations have been performed for a model representative of the MUSE-4 experiments currently underway in the MASURCA facility.*

It has been found that the high-energy neutrons (E_n > 20 MeV) born from spallation, even though they represent only about 17% of the total neutrons, contribute for a large fraction (50%) to φ^* and to the total number of fission neutrons produced in the core. It has also been found that codes such as ERANOS, which do not take into account neutrons with energies higher than 20 MeV, largely underestimate φ^*.

I. INTRODUCTION

Accelerator Driven Systems (ADS) (Ref. 1) are being investigated as a possible means for reducing the long-term radiotoxicity of the spent reactor fuel. In principle, the sub-criticality of ADS allows for dedicated cores with a much higher concentration of minor actinides than what is acceptable in critical reactors. Those dedicated cores could achieve high transmutation rates. Research done on ADS indicates that a radiotoxicity reduction factor of 50 to 100 is theoretically possible (Ref. 2).

In an ADS, neutrons generated by an intense external source, usually spallation reactions in a heavy metal target, are supplied to a sub-critical reactor core. This idea is being investigated in the MASURCA experimental facility at CEA Cadarache in the framework of the MUSE experiments (MUltiplication avec Source Externe) (Refs. 3, 4 and 5). Different configurations and several sub-critical levels are being studied.

The on-going MUSE-4 experiments do not use a spallation source. Instead, a high-intensity pulsed neutron generator GENEPI, constructed by CNRS/ISN/Grenoble, is being used to accelerate a 250 keV deuteron beam towards either a deuterium target or a tritium target, producing well-characterized neutron sources via fusion reactions.

In a previous study (Ref. 8), we investigated spallation neutron source effects in a MUSE-4 type sub-critical core coupled to a 1000 MeV proton beam, in particular the contribution of high-energy neutrons (E_n > 20 MeV) to the source efficiency (φ^*). The objective of the present study is to complement this past work. Additional numerical simulations have been performed with the Monte Carlo code MCNPX (Ref. 6). The results have been compared to those obtained with ERANOS (Ref. 7), the CEA reference deterministic code system for fast reactor analyses.

* E-mail: per@neutron.kth.se

A description of the MUSE-4 model, the MCNPX and ERANOS codes and the spallation neutron source used in this study is given in Section II. In Section III, the specific procedure used for calculating φ^* with MCNPX and ERANOS is described. A decomposition of the spallation source is performed and analysed. The results of the MCNPX and ERANOS simulations are compared.

II. DESCRIPTION OF THE MUSE-4 MODEL, THE CALCULATION CODES AND THE SPALLATION NEUTRON SOURCE USED IN THIS STUDY

II.A. *The Muse-4 Model*

A homogeneous model representing one of the sub-critical configurations (SC3) planned in the MUSE-4 experiments (k_{eff} = 0.95) has been studied. The geometry of the model is shown in Fig. 1. The fuel is MOX fuel with 72% U-238, 21% Pu-239 and 5% Pu-240 plus small amounts of some other actinides. The fuel is homogeneously distributed together with the Na-coolant (Ref. 8). The axial (z-direction) dimension of the fuel is 60.96 cm, except in a 21.2 cm wide channel above and below the lead buffer and the accelerator tube (in the y direction), where it was extended by 10.16 cm. The sodium-steel reflector ends at z = ±61.76 cm. There is also a 10.16 thick axial shield (not shown in the figure) above and below the Na/SS reflector. The overall dimensions of the whole model, including the reflector and the shields, are 159 cm x 169.6 cm x 143.84 cm.

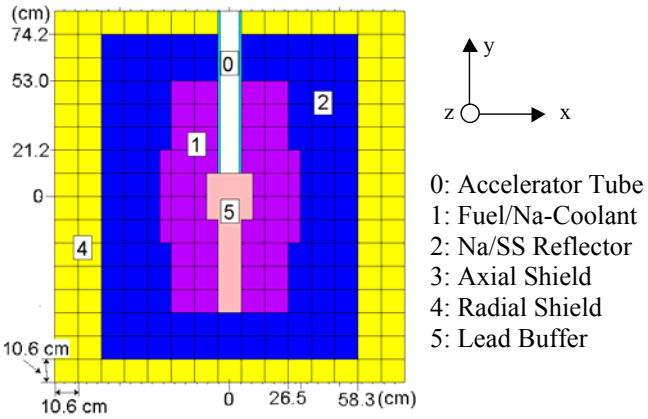

Fig. 1. x-y cross-sectional view of the model of the MUSE-4 sub-critical configuration (k_{eff} = 0.95).

II.B. *The Calculation Codes*

II.B.1. MCNPX

MCNPX is an extended version of MCNP where the major capabilities of LAHET (Ref. 9) and MCNP-4B (Ref. 10) have been merged together. In MCNP, particle transport relies entirely on nuclear data contained in externally supplied cross section tables (E_n < 20 MeV), which are derived from evaluated nuclear data files. In LAHET, on the other hand, particle transport is accomplished by using various theoretical physics models embedded in the code, covering the energy range up to several GeV. In MCNPX, the table-based data are used whenever they exist, as such data are known to yield the best results. When they do not exist, the code built-in physics models are used.

Several physics models are available for high-energy transport in MCNPX. In the first stage, in which the incident particles interact with the individual nucleons via particle-particle cross sections, the Intranuclear Cascade (INC) and Multistage Pre-equilibrium (Ref. 11) Models are used. The INC model used in this study is the Bertini package (Ref. 12). In the second stage the nucleus undergoes either evaporation (emitting neutrons and light ions) or fission, while in the final stage the excited nucleus decays by gamma emission, with energies described by a decay library (PHTLIB).

In this study, all simulations performed with MCNPX relied on the same evaluated nuclear data library, namely ENDF/B-VI.6.

II.B.2. ERANOS

ERANOS is a deterministic fast reactor code system developed by CEA in collaboration with other R&D organizations (Ref. 7). It uses cross-section libraries based on the JEF2.2 evaluated file. The ERANOS code system is well validated for classical sodium-cooled fast reactors. This validation has been recently extended to plutonium burning cores with steel-sodium reflectors and high Pu-content. However, the code is not yet fully validated for systems characterized by large sub-criticalities and the presence of high-energy neutrons from spallation.

In ERANOS, *1-D* cell or *2-D* subassembly calculations are performed with the ECCO code, while core calculations can be performed with different *2-D* or *3-D*, diffusion or transport theory modules. In this study, the two-dimensional S_n transport code BISTRO (Ref. 13) was used.

II.C. *Description of the Spallation Source and the Primary Spallation Neutrons*

The MCNPX simulations calculating the efficiency of the spallation source neutrons were divided into two steps. In the first simulation, a large number of protons (1000 MeV) were accelerated towards the lead target (Fig. 2). The protons were uniformly distributed across the beam of radius 2 cm. The angular, energy and spatial distributions of all neutrons that were created directly from the spallation interactions (primary spallation neutrons) were recorded. After that the neutron trajectories were immediately terminated. This procedure produces the spectrum of primary spallation neutrons, i.e. no secondary neutrons are included.

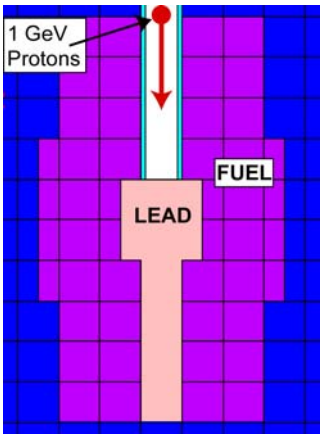

Fig. 2. 1000 MeV protons accelerated towards the lead target creating neutrons via spallation interactions. The generated primary neutrons are "frozen" at the moment when they are created, and emitted as fixed source neutrons in a separate simulation.

In the second step, these primary spallation neutrons were supplied to the MCNPX code as fixed source neutrons for separate simulations and the source efficiency was determined.

The spatial distribution where the primary neutrons were created was found to be rather limited. Axially, most of the neutrons were emitted in the upper part of the lead target (77% within the first 20 cm, see Fig. 3A). The radial distribution was found to be very peaked around the axis of the incident proton beam, about 98% of the neutrons were created within a 3 cm radius (Fig. 3B).

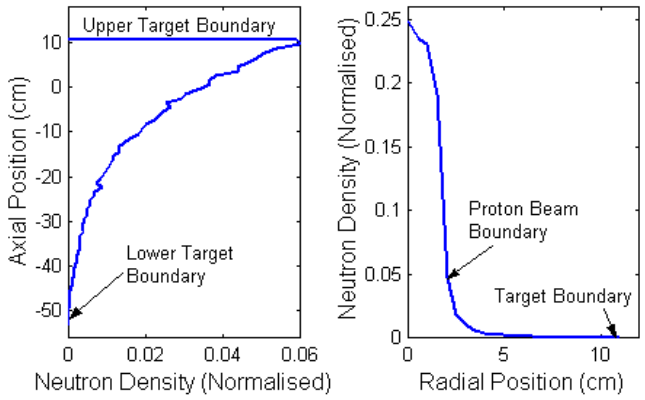

Fig. 3. A) Axial distribution of the primary spallation neutrons. B) Radial distribution of the primary spallation neutrons.

The energy distribution of the primary neutrons produced by the 1000 MeV protons is shown in Fig. 4. We note that 16.8% of the neutrons have energies higher than 20 MeV and 3.3% of them higher than 150 MeV, and that the neutrons with very high energy are mainly emitted in the forward direction of the proton beam, as expected.

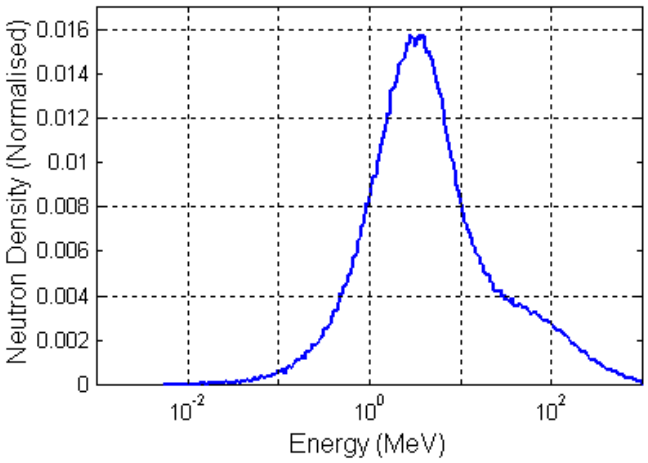

Fig. 4. Energy spectrum of the primary spallation neutrons created by the 1000 MeV protons.

There were about 14.5 primary spallation neutrons produced per 1000 MeV proton. This value should be compared to the total number of neutrons produced in the lead target, i.e. around 21 neutrons per proton. Thus, almost a third of the neutrons that exit the lead target and enter into the fuel are secondary neutrons, most of them created in neutron spallation reactions and *(n,xn)*-reactions.

It should be noted that, when calculating φ^* for a spallation system, the results are directly dependent on the definition of the neutron source. Other source definitions are possible (Refs. 14 and 15), which will result in different meanings and values for φ^*.

III. SOURCE EFFICIENCY

III.A. *Definition of φ^**

The neutron flux distribution ϕ_s in a sub-critical core is the solution of the inhomogeneous balance equation:

$$\boldsymbol{A}\phi_S = \boldsymbol{F}\phi_S + S \tag{1}$$

where $\boldsymbol{F}$ is the fission production operator, $\boldsymbol{A}$ is the net neutron loss operator and S is the external source. The quantity φ^*, which represents the relative efficiency of external source neutrons, is defined as the ratio of the average importance of the external source neutrons to the average importance of the fission neutrons (Ref. 1), i.e.:

$$\varphi^* = \frac{\dfrac{<\phi^*_0, S>}{<S>}}{\dfrac{<\phi^*_0, \boldsymbol{F}\phi_S>}{<\boldsymbol{F}\phi_S>}} \tag{2}$$

where

ϕ^*_0 = The adjoint flux (the everywhere positive solution of $\boldsymbol{A}^*\phi^*_0 = 1/k_{eff} \cdot \boldsymbol{F}^*\phi^*_0$), which provides a measure of neutron importance.

$<\boldsymbol{F}\phi_s>$ = Total production of neutrons by fission.

$<S>$ = Total production of neutrons by the external source.

In the above formula, the brackets imply integration over space, angle and energy.

As some of the integrals in Eq. (2) cannot be directly calculated with MCNPX, another procedure was sought to compute φ^*. By using the balance equation [Eq. (1)], the properties of the adjoint flux ϕ_0^*, the $\boldsymbol{A}$, $\boldsymbol{F}$ operators and their adjoints $\boldsymbol{A}^*$, $\boldsymbol{F}^*$, the source efficiency can be expressed equivalently as:

$$\varphi^* = \left(\frac{1}{k_{eff}} - 1\right) \cdot \frac{<\boldsymbol{F}\phi_S>}{<S>} \tag{3}$$

Eq. (3) is a simple formula relating the total fission neutron production $<\boldsymbol{F}\phi_s>$ to the external source, φ^* and reactivity $(1 - 1/ k_{eff})$. It shows that, for given values of k_{eff} and $<S>$, the larger φ^* the larger the fission power produced in the system.

The quantities in the right hand side of Eq. (3) are standard outputs from MCNPX.

III.B. *Decomposition of the Spallation Source*

Most reactor codes take into account only neutrons with energies lower than 20 MeV. However, a significant fraction of the neutrons produced by spallation have energies higher than 20 MeV (Fig. 4). The contribution of those high-energy neutrons to the source efficiency needs to be investigated. For this, the spallation source was artificially split into two "low-energy" bins (S_1 from 0 to 5 MeV and S_2 from 5 to 20 MeV) and two "high-energy" bins (S_3 from 20 to 150 MeV and S_4 from 150 to 1000 MeV), as explained in Ref. 8.

In order to derive a formula for the low- and high-energy contributions to the source efficiency, we start from Eq. (3), applied to each source bin

$$\varphi^*_i = \left(\frac{1}{k_{eff}} - 1\right) \cdot \frac{<\boldsymbol{F}\phi_i>}{<S_i>} \tag{4}$$

where

ϕ_i = Flux resulting from each source bin alone ($S_1 \rightarrow \phi_1$, $S_2 \rightarrow \phi_2$ etc.).

Since $<\boldsymbol{F}\phi_T> = \sum_{i=1}^{4} <\boldsymbol{F}\phi_i>$, the following relationship for the decomposition of φ^* is readily obtained:

$$\varphi^*_T = \sum_{i=1}^{4} \varphi^*_i \cdot \frac{<S_i>}{<S_T>} \tag{5}$$

where

φ^*_T = Efficiency of the total source.

φ^*_i = Efficiency of each source bin alone.

III.B.1. Calculations Performed with MCNPX

The φ^*_i results obtained from the MCNPX simulations are listed in Table I. As expected, for the first low-energy bin, φ^*_i is relatively low ($\varphi^*_1 = 1.24$). For the second bin, it is found to be higher ($\varphi^*_2 = 1.63$), since many of the neutrons have energies above the lead *(n,2n)*-cross section threshold (ref. 8). For the two high-energy parts, φ^*_i is very high ($\varphi^*_3 = 4.79$ and $\varphi^*_4 = 13.9$), which is the consequence of fissions induced by secondary neutrons born from *(n,xn)*-

reactions and neutron spallation interactions. The statistical relative 1σ error estimates in the φ^* values are about 1 %.

TABLE I

MCNPX Results for the Decomposition of the Spallation Source, Obtained for the MUSE-4 Model (k_{eff} = 0.95013 ± 14 pcm).

Source Bin	Energy intervals (MeV)	$\frac{<S_i>}{<S_T>}$ A	$\frac{<\boldsymbol{F}\phi_i>}{<S_i>}$ B	φ^*_i	$\varphi^*_i \cdot \frac{<S_i>}{<S_T>}$ C
S_1	0 - 5	0.592	23.5	1.24	0.736 (33 %)
S_2	5 - 20	0.240	31.1	1.63	0.390 (17 %)
S_3	20 - 150	0.135	91.3	4.79	0.647 (29 %)
S_4	150 - 1000	0.033	264.3	13.9	0.458 (21 %)
					Sum = 2.23
S_T D	0 - 1000	1.0	42.2	2.21	

The superscripts *A*, *B*, *C* and *D* in Table I stand for:

A: Fraction of the total number of source neutrons in each energy bin (compare Fig. 4).

B: Neutrons produced by fission in the core, per external source neutrons from bin *i*.

C: Contribution to total φ^* (Product of column 3 and column 5).

D: Simulation with the total source.

It is also seen in Table I that the two high-energy parts (16.8% of the total number of source neutrons), contribute for about 50% of the total φ^*, and the highest energy part alone (3.3% of the total number of source neutrons) for more than 20%. The sum of the contributions to φ^* from the four different parts in the rightmost column, according to Eq. (5), is 2.23, which is in agreement with the value obtained from the simulation with the total source (φ^*_T = 2.21). Comparisons with additional calculations (Ref. 8) show that this value is slightly higher than the φ^*-value obtained for a *(d,t)*-fusion source, coupled to the same model ($\varphi^*_{d,t}$ = 2.12), and much higher than for a *(d,d)*-source ($\varphi^*_{d,d}$ = 1.34).

The rather high average number of fission neutrons produced per source neutron for the two high-energy bins (91 and 264, respectively) might seem surprising at first. The explanation for this is that most of the high-energy neutrons from the spallation source have already been multiplied in the lead (most of them via secondary neutron spallation and *(n,xn)*-reactions) *before* they enter into the fuel. Each of them gives birth to a number of lower-energy neutrons, which then leak out of the lead and induce fission chain reactions in the fuel. Additional simulations in which the lead target alone was kept show that only about 5 % of the neutrons leaking out of the lead have energies higher than 20 MeV and about 1% of them higher than 150 MeV.

We conclude that, although neutron transport in the fuel is largely dominated by neutrons with low energies (E_n < 20 MeV) which can be well simulated with a number of classical calculation codes such as MCNP and ERANOS, high-energy neutrons contribute significantly to φ^*. Further investigating these high-energy effects would be made easier by extending the neutron data libraries of existing codes from 20 MeV to at least 150 MeV.

III.B.2. Comparisons between MCNPX and ERANOS

In practice, many hybrid system core studies rely on deterministic codes such as ERANOS, which do not model neutrons with energies above 20 MeV. It is therefore interesting to compare the predictions of such codes with MCNPX. While only small differences are expected in reactivity and power shape predictions (see Fig. 5), the results of the previous section suggest that a rather large impact is anticipated on φ^*.

To verify this conjecture, a small benchmark was defined and calculated with both MCNPX and ERANOS. This benchmark is a simplified two-dimensional *R-Z* version of the MUSE-4 model described in Fig. 1. The distribution of the primary source neutrons was slightly simplified to make it possible to use exactly the same sources in both ERANOS and MCNPX.

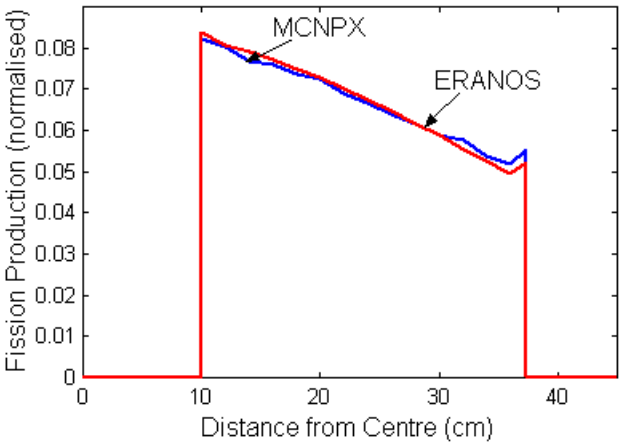

Fig. 5. Radial power profiles computed by MCNPX and ERANOS.

There are at least two ways of calculating φ^* with ERANOS. The first possibility is to use Eq. 2. However, this requires an adjoint calculation. Another, simpler way is to use Eq. 3, which may also be written as:

$$\varphi^* = \frac{1/k_{eff} - 1}{1/k_s - 1} \qquad (6)$$

where $k_s = < \boldsymbol{F}\phi_s > / < \boldsymbol{A}\phi_s >$.
We chose this second alternative.

As can be seen in Table II, ERANOS produces values of φ^* in fairly good agreement with MCNPX for the two low-energy bins S_1 and S_2, in spite of differences between the nuclear datasets used by the two codes. The relative statistical 1σ error estimates in the φ^* values for the MCNPX-calculations are less than 1%.

TABLE II
MCNPX and ERANOS Results for a Simplified Two-Dimensional MUSE-like Model ($k_{eff} \approx 0.95$).

Source Bin	Energy intervals (MeV)	$\frac{< S_i >}{< S_T >}$	φ^*_i	
			MCNPX	ERANOS
S_1	0 - 5	0.592	1.20	1.14
S_2	5 - 20	0.240	1.56	1.49
S_3	20 - 150	0.135	4.56	-
S_4	150 - 1000	0.033	14.6	-
S_T	0 - 1000	1.0	2.17	1.42[A]

[A] When simulating the total source with ERANOS, all neutrons above 20 MeV (16.8%) were placed in the highest energy group (14.2 to 19.6 MeV).

However, since the ERANOS libraries are currently limited to neutrons below 20 MeV, the value of φ^* for the total source is much lower (φ^*_{ERANOS} = 1.42) than the MCNPX value (φ^*_{MCNPX} = 2.17). A large fraction (~ 35%) of the total value of φ^* is actually not reflected in the ERANOS results. This is something one should bear in mind when calculating φ^* for a spallation source with ERANOS or any other "low"-energy reactor code.

IV. CONCLUSIONS

Numerical simulations have been performed with MCNPX and ERANOS to investigate the neutronic properties of a sub-critical model (k_{eff} = 0.95) representative of the on-going MUSE-4 experiments, coupled to a spallation source (1000 MeV protons impinging on a lead target). The system has been studied in terms of source efficiency (φ^*).

The efficiency of the total spallation source was found to be 2.21, which could be compared to φ^* for a *(d,t)*- and a *(d,d)*-source, coupled to the same system ($\varphi^*_{d,t}$ = 2.12 and $\varphi^*_{d,d}$ = 1.34, respectively). To analyse this rather high value of φ^*, the spallation source was artificially split into four energy bins and the efficiency of each bin was determined. It was found that the two high-energy bins (E_n > 20 MeV) contribute for about 50% to φ^* and to the total number of fission neutrons produced in the core. This can be explained by the fact that primary neutrons born with high energy from spallation give birth to a large number of lower-energy

neutrons, which in turn induce fissions. This finding indicates the need for extending reactor analysis code capabilities above 20 MeV for more detailed investigations of high-energy spallation neutron effects.

Comparisons of ERANOS and MCNPX calculations of φ^* were found to be in good agreement for the energy bins below 20 MeV. However, as ERANOS does not take into account neutrons above 20 MeV, it largely underestimates the total value of φ^*. This effect should be remembered when calculating φ^* with reactor codes that do not account for neutrons above 20 MeV.

AKNOWLEDGEMENTS

This research work is supported and partly funded by the Swedish Centre of Nuclear Technology, SKB AB (Sweden), CEA/Cadarache (France) and the European Commission, DGRTD, under Contract # FIKW-CT-2000-00063.

REFERENCES

1. M. SALVATORES, "Accelerator Driven Systems (ADS), Physics Principles and Specificities," J. Phys. IV France 9, pp. 7-17 –7-33 (1999).

2. M. DELPECH et al., "The Am and Cm Transmutation – Physics and Feasability," *Proc. Int. Conf. Future Nuclear Systems, GLOBAL'99,* August 30-September 2, 1999, Jackson Hole, Wyoming, American Nuclear Society (1999).

3. M. SALVATORES, M. MARTINI, I. SLESSAREV, "MUSE-1: A first Experiment at MASURCA to Validate the Physics of Sub-Critical Multiplying Systems Relevant to ADS," Kalmar, Sweden, June 3-7 (1996).

4. R. SOULE, M. SALVATORES, R. JACQMIN, "Validation of Neutronic Methods Applied to the Analysis of Fast Sub-Critical Systems: The MUSE-2 Experiments," GLOBAL'97, page 639 (1997).

5. J. F. LEBRAT et al., "Experimental Investigation of Multiplying Sub-Critical Media in Presence of an External Source Operating in Pulsed or Continuous Mode: The MUSE-3 Experiment," ADTTA'99 (1999).

6. L. S. WATERS, "MCNPX™ User´s Manual – Version 2.1.5," Los Alamos National Laboratory, November 14, (1999).

7. J.Y. DORIATH et al, "ERANOS 1: The Advanced European System of Codes for Reactor Physics Calculation," *Int. Conf. on Mathematical Methods and Super Computing in Nuclear Application*, 19-23 April 1993, Kongresszeutrum, Karlsruhe, Germany (1993).

8. P. SELTBORG, R. JACQMIN, "Investigation of Neutron Source Effects in Sub-Critical Media and Application to a Model of the MUSE-4 Experiments," *Int. Meeting on Mathematical Methods for Nuclear Applications, Mathematics and Computation*, September 9-13, 2001, Salt Lake City, Utah, USA (2001).

9. R. E. PRAEL, H. LICHTENSTEIN, "User Guide to LCS: The LAHET Code System," LA-UR-89-3014, Los Alamos National Laboratory (1989).

10. MCNP™ – A General Monte Carlo N-Particle Transport Code – Version 4B," LA-12625-M, J. F. BRIESMEISTER, Ed., Los Alamos National Laboratory, (1997).

11. R. E. PRAEL R, M. BOZOIAN, "Adaptation of the Multistage Pre-equilibrium Model for the Monte Carlo Method (1)," LA-UR-88-3238, Los Alamos National Laboratory Report, September (1998).

12. H. W. BERTINI, Phys. Rev. 131, 1801, (1969).

13. G. PALMIOTTI et al, "BISTRO Optimized Two Dimensional Sn Transport Code," *Topical Meeting on Advances in Reactor Physics, Mathematics and Computation*, April 1987, Paris, France (1987).

14. K. TUCEK et al., "Source Efficiency in an Accelerator-Driven System with Burnable Absorbers,", *Int. Conf. on Back-End of the Fuel Cycle: From Research to Solutions, GLOBAL 2001*, Paris, France (2001).

15. S. ATZENI et al., "Statistical Fluctuations in Monte Carlo Simulations of a Sub-Critical System," CERN-LHC-97-012-EET, CERN (1997).